Research Article

INTERNATIONAL JOURNAL OF ADVANCED ROBOTIC SYSTEMS

International Journal of Advanced Robotic Systems
May-June 2018: 1–10

DOI: 10.1177/1729881418778228
journals.sagepub.com/home/arx
SAGE

Formation control for car-like mobile robots using front-wheel driving and steering

Haojie Chen[1], Hong'an Yang[1], Xu Wang[1] and Ting Zhang[2]

Abstract

To solve the problem of front wheels being jammed due to the passive trajectory tracking of the conventional car-like robot in the leader–follower formation control, we propose a novel car-like robot with the integration of front-wheel driving and steering. We establish its kinematic model, then analyze its controllability via the method of chained form system, and design the trajectory-tracking controller via the backstepping method. Simulations and experimental results validate our algorithm. This novel car-like robot with the integration of front-wheel driving and steering system not only avoids the jamming in the formation motion, but also owes the advantages of compacter structure, lighter body, and lower energy consumption.

Keywords

Formation control, trajectory tracking, car-like robot, front-wheel driving and steering, chained form system, backstepping

Date received: 17 October 2017; accepted: 26 April 2018

Topic: Mobile Robots and Multi-Robot Systems
Topic Editor: Nak-Young Chong
Associate Editor: Chang-bae Moon

Introduction

The problem of controlling formations of multiple mobile robots has drawn a considerable amount of research efforts.[1] There are various techniques available in the literature for the formation control of mobile robots, such as behavior-based approach,[2] virtual structure approach,[3] and leader–follower approach.[4] The leader–follower approach has been the most popular one due to its ease of implementation and analysis. In the leader–follower approach, one robot (the leader) moves along a predefined trajectory, while the rest of the robots (the follower robots) are in a passive situation where they have to keep track of the leader robot and maintain the desired distance and bearing angles.

There are also many types of mobile robot in leader–follower formation control, for example, differential-drive mobile robot,[5] omnidirectional mobile robot,[6] unmanned ground vehicle,[7] and car-like mobile robot.[8–10] Car-like mobile robot stands out in some environments because of its stability and the ability of heavy load. To our knowledge, the type of car-like robots in leader–follower formation control is mainly the front-wheel steering and rear-wheel driving.[9,10] When considering the problem of accurate trajectory tracking, the conventional car-like mobile robots with front-wheel steering and rear-wheel driving are quite difficult to control. In fact, the front

[1] School of Mechanical Engineering, Northwestern Polytechnical University, Xi'an, China
[2] Hytera Communications Corporation Limited, Shenzhen, China

Corresponding author:
Hong'an Yang, School of Mechanical Engineering, Northwestern Polytechnical University, Xi'an 710072, China.
Email: yhongan@nwpu.edu.cn

wheels may easily become jammed at steering angles nearly $\pm 90^\circ$ due to the passive following, causing the tracking failure of the follower robots and distortion of the formation.

The focus of this article is on solving the jamming problem of front wheels, and we change the structure of the conventional car-like robot and propose the formation control of a team of car-like mobile robots with front-wheel driving and steering. In addition, this novel car-like robot with the integration of front-wheel driving and steering system also owes the advantages of more compact structure, smaller body, and lower energy consumption, which make the robots or the formation move through the narrow environment effectively. At the same time, this mode can move on rough terrains with ease and good maneuverability.

Each type of robot has different kinematic models, which affect the result of motion control of a mobile robot and trajectory tracking of follower robots in formation control. The new robot is different from conventional car-like robots, where front wheels are the driving wheels and the steering wheels. From the modeling point of view, the kinematics of the robot should be considered and its controllability needs to be analyzed. Moreover, the robot with front-wheel driving and steering is first applied in leader–follower formation motion, and the trajectory tracking controller must be designed for follower robots to achieve and maintain the formation.

The design of tracking controller for the new car-like robot has been a great challenge. The methods of solving the trajectory tracking problem include the backstepping method,[9,10] the adaptive tracking control,[7,11] and a control algorithm designed for general nonholonomic systems in chained form.[12–14] The class of nonholonomic system in chained form has been studied as a benchmark example.[13,15] It is well known that many mechanical systems with nonholonomic constraints can be converted to chained form under coordinate change and state feedback. In addition, the backstepping method is a typical nonlinear control approach that can be used to design a controller recursively and handle high-order controllers effectively. The car-like mobile robot is a typical nonlinear system with nonholonomic constraints. Therefore, the new controller based on the chained form system and the backstepping method is designed to achieve the formation in this article.

The article is organized as follows. The "Kinematic models and controllability analysis of the novel robot" section establishes the new geometry of the car-like robot and presents the process of how to verify the controllability of the new car-like robot. The "Trajectory tracking controller design" section describes the trajectory error of follower robots and how the follower robots' controller is designed using the chained form system and the backstepping method. The section "Results and discussions of the simulations and experiments" provides the simulations and the experimental results.

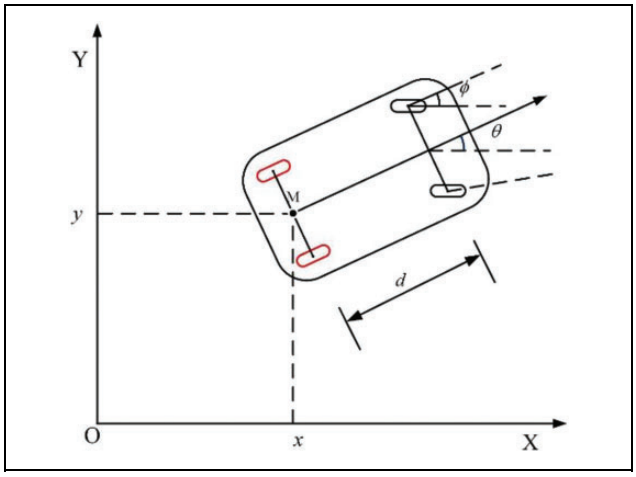

Figure 1. The geometry of the conventional car-like robot with rear-wheel driving.

Kinematic models and controllability analysis of the novel robot

Kinematic model of the conventional car-like robot with front-wheel steering and rear-wheel driving

The geometry of the conventional car-like robot is depicted in Figure 1. M is located at the middle point between the right and left driving wheels, and d is the distance from the rear axle to the front of the mobile robot. The posture of the robot can be $p = (x, y, \theta, \phi)^T$ in an inertial Cartesian frame, where (x, y) is the Cartesian coordinates of the reference point M, θ is the heading angle of the robot with respect to the x-axis, and ϕ is the steering angle relative to the robot body.

Based on the work of Chen and Jia,[5] the rear wheel of conventional robot satisfies the conditions of pure rolling and nonslipping. This nonholonomic constraint can be written as follows

$$\begin{bmatrix} \sin\theta & -\cos\theta & 0 & 0 \end{bmatrix} \begin{bmatrix} \dot{x} \\ \dot{y} \\ \dot{\theta} \\ \dot{\phi} \end{bmatrix} = 0 \qquad (1)$$

From equation (1), the kinematic model of the conventional robot with front-wheel steering and rear-wheel driving is written as

$$\begin{bmatrix} \dot{x} \\ \dot{y} \\ \dot{\theta} \\ \dot{\phi} \end{bmatrix} = \begin{bmatrix} \cos\theta \\ \sin\theta \\ \tan\phi/d \\ 0 \end{bmatrix} \nu + \begin{bmatrix} 0 \\ 0 \\ 0 \\ 1 \end{bmatrix} \omega \qquad (2)$$

where ν and ω are denoted as the linear velocity and steering velocity inputs of the nonholonomic car-like robot, respectively.

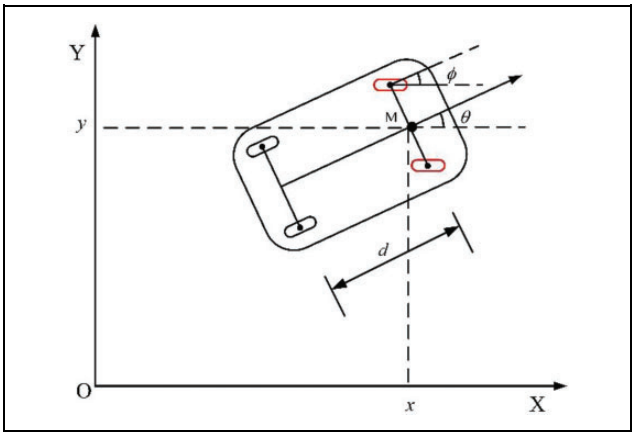

Figure 2. The geometry of the novel car-like robot with front-wheel driving and steering.

Kinematic model of the novel car-like robot with front-wheel driving and steering

The geometry of the novel car-like robot with front-wheel driving and steering is depicted in Figure 2.

The front wheels of the novel robot satisfy the conditions of pure rolling and nonslipping. This nonholonomic constraint can be written as follows

$$\begin{bmatrix} \sin(\theta+\phi) & -\cos(\theta+\phi) & 0 & 0 \end{bmatrix} \begin{bmatrix} \dot{x} \\ \dot{y} \\ \dot{\theta} \\ \dot{\phi} \end{bmatrix} = 0 \quad (3)$$

From equation (3), the kinematic model of the robot with front-wheel driving and steering is written as

$$\begin{bmatrix} \dot{x} \\ \dot{y} \\ \dot{\theta} \\ \dot{\phi} \end{bmatrix} = \begin{bmatrix} \cos(\theta+\phi) \\ \sin(\theta+\phi) \\ \sin\phi/d \\ 0 \end{bmatrix} \nu + \begin{bmatrix} 0 \\ 0 \\ 0 \\ 1 \end{bmatrix} \omega \quad (4)$$

Note that when ϕ is nearly $\pm 90^\circ$ in equation (2), $\dot{\theta} = \nu \times \tan\phi/d$ will diverge, but in equation (4), $\dot{\theta} = \nu \times \sin\phi/d$ is bounded and the front wheel is not jammed, and the robot can still pivot about its rear wheel. The new structure helps to avoid the robot becoming jammed at ϕ nearly $\pm 90^\circ$, so we employ it in formation control to avoid the jamming that occurs in the process of tracking the desired trajectories for follower robots.

Controllability analysis of the novel car-like robot

In order to achieve the formation, the new robot in formation should be controllable. Therefore, we must analyze the controllability of the robot. The chained form is a canonical form for a class of nonholonomic systems, and if a system can be transformed into a chained form, it is controllable.[13] However, it is difficult to find a conversion from a kinematic model to the chained form, the paper[14] shows that all the systems with the triangular structure enjoy the convertibility kinematic model. Based on the work of Nakamura et al.,[14] we transform equation (4) into a triangular structure as follows

$$\begin{cases} \dot{q}_1 = \nu_1 \\ \dot{q}_2 = \omega \\ \dot{q}_3 = f_3(\underline{q}_2)\cdot\nu_1 \\ \dot{q}_4 = f_4(\underline{q}_3)\cdot\nu_1 \end{cases} \quad (5)$$

where $\nu_1 = \nu\cos(\theta+\phi)$, $(q_1 \quad q_2 \quad q_3 \quad q_4)^T \triangleq (x \quad \phi \quad \theta \quad y)^T$ is the state variables, and $f_3(\underline{q}_2) = \frac{\sin\phi\sec(\theta+\phi)}{d}$ and $f_4(\underline{q}_3) = \tan(\theta+\phi)$ are smooth functions.

Assume that at $q = p_0$ on the configuration manifold, we have

$$\left.\frac{\partial f_i(\underline{q}_{i-1})}{\partial q_{i-1}}\right|_{q=p_0} \neq 0, \quad \forall i \in \{3,4\} \quad (6)$$

Then, at the neighborhood of $q = p_0$, a coordinate transformation from the triangular structure (equation (5)) to the chained form is given by

$$\begin{cases} z_4 = h_4(q_4) = q_4 = y \\ z_3 = h_3(q_3) = \dfrac{\partial h_4(q_4)}{\partial q_4}\cdot f_4(q_3) = \tan(\theta+\phi) \\ z_2 = h_2(q_2) = \dfrac{\partial h_3(q_3)}{\partial q_3}\cdot f_3(q_2) + \dfrac{\partial h_3(q_3)}{\partial q_4}\cdot f_4(q_3) = \dfrac{1}{d}\sin\phi\sec^3(\theta+\phi) \\ z_1 = h_1(q_1) = x \end{cases} \quad (7)$$

and the state feedback is

$$\begin{cases} u_1 = \nu_1 = \nu\cos(\theta + \phi) \\ u_2 = \dot{z}_2 = \dfrac{\partial h_2(q_2)}{\partial q_2}\dot{q}_2 + \dfrac{\partial h_2(q_2)}{\partial q_3}\dot{q}_3 + \dfrac{\partial h_2(q_2)}{\partial q_4}\dot{q}_4 \\ \quad = \dfrac{[3\sin\phi\sin(\theta+\phi)\sec^4(\theta+\phi) + \cos\phi\sec^3(\theta+\phi)]\cdot\omega}{d} + \dfrac{3\sin(\theta+\phi)\sin^2\phi\sec^4(\theta+\phi)\cdot\nu}{d^2} \end{cases} \tag{8}$$

where $h_n(q_n)$ is any smooth function which satisfies

$$\left.\frac{\partial h_n(q_n)}{\partial q_n}\right|_{q=p_0} \neq 0 \tag{9}$$

Then, according to the study by Jiang and Nijmeijer,[13] the triangular structure (equation (5)) is transformed into chained form as follows

$$\begin{cases} \dot{z}_1 = u_1 \\ \dot{z}_2 = u_2 \\ \dot{z}_3 = z_2 \cdot u_1 \\ \dot{z}_4 = z_3 \cdot u_1 \end{cases} \tag{10}$$

where $u = (u_1, u_2)^T$ is the state feedback and $Z = (z_1 \quad z_2 \quad z_3 \quad z_4)^T$ is the current state of robot after transformation, respectively.

Based on the abovementioned transformation, the kinematic model (equation (4)) is converted to a chained form (equation (10)); thus, we have verified that the new car-like robot is controllable, that is, there exists an appropriate controller for it to achieve the formation.

Trajectory tracking controller design

Based on the abovementioned controllability analysis of the new nonholonomic car-like robot, we know that there exists an appropriate controller for these nonholonomic robots to move along the desired trajectory. In this section, we focus on how to design the trajectory-tracking controller for the new robots to form the leader–follower formation. First, we establish the leader–follower formation control framework, and then transform the tracking error model into chained form. Finally, an effective tracking controller for follower robots is designed recursively based on the backstepping method.

The leader–follower formation control framework

Considering a group of n nonholonomic wheeled mobile robots with front-wheel driving and steering, Figure 3(b) shows the tracking model of leader–follower formation. We denote $l_{iL} \in R$ as the actual distance between the follower robot R_{i} and the leader robot R_{L}. $l_{iL}^d \in R$ is the desired distance. $\varphi_{iL} \in [-\pi\ \pi]$ is the actual bearing angle from the orientation of the follower robot to the axis connecting R_{i} and R_{L}. ${\varphi_{iL}}^d \in [-\pi\ \pi]$ is the desired bearing angle.

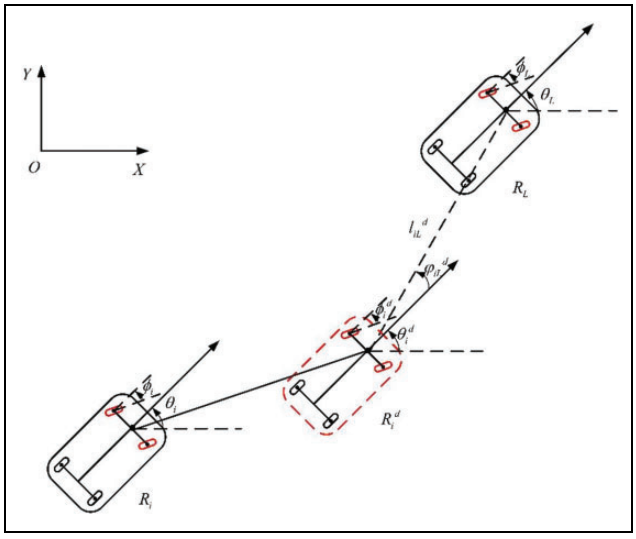

Figure 3. The leader–follower formation of car-like robots with front-wheel driving and steering.

The follower robot's desired posture $p_i^d = (x_i^d, y_i^d, \theta_i^d, \phi_i^d)^T$ with respect to the leader can be obtained using

$$\begin{cases} x_i^d = x_L - l_{iL}^d\cos(\theta_L + \varphi_{iL}^d) \\ y_i^d = y_L - l_{iL}^d\sin(\theta_L + \varphi_{iL}^d) \\ \theta_i^d = \theta_L \\ \phi_i^d = \phi_L \end{cases} \tag{11}$$

where $(x_L, y_L, \theta_L, \phi_L)^T$ is the posture of the leader.

Comparing the follower robot's desired posture $p_i^d = (x_i^d, y_i^d, \theta_i^d, \phi_i^d)^T$ with the follower robot's current posture $p_i = (x_i, y_i, \theta_i, \phi_i)^T$, the tracking error E_i in a coordinate system can be described as

$$E_i = p_i^d - p_i = \begin{bmatrix} x_e \\ y_e \\ \theta_e \\ \phi_e \end{bmatrix} = \begin{bmatrix} x_i - x_i^d \\ y_i - y_i^d \\ \theta_i - \theta_i^d \\ \phi_i - \phi_i^d \end{bmatrix} \tag{12}$$

The transformation of tracking error model in chained form

We denote every follower R_{i} with the same kinematic model of the chained form

$$\begin{cases} \dot{z}_{i1} = u_{i1} \\ \dot{z}_{i2} = u_{i2} \\ \dot{z}_{i3} = z_{i2} \cdot u_{i1} \\ \dot{z}_{i4} = z_{i3} \cdot u_{i1} \end{cases} \tag{13}$$

$u = (u_{i1}, u_{i2})^T$ is the state feedback and $Z_{ie} = (z_{i1e}, z_{i2e}, z_{i3e}, z_{i4e})^T$ is the current state of the ith follower robot R_{i} after transformation, respectively. Because we verify the controllability of the robot using the chained form, we should transform the tracking error model (equation (12)) into the chained form $Z_{ie} = (z_{i1e}, z_{i2e}, z_{i3e}, z_{i4e})^T$ and then, design the controller

$$\begin{cases} z_{i1e} = z_{i1} - {z_{i1}}^d \\ z_{i2e} = z_{i2} - {z_{i2}}^d \\ z_{i3e} = z_{i3} - {z_{i3}}^d \\ z_{i4e} = z_{i4} - {z_{i4}}^d \end{cases} \tag{14}$$

where ${Z_i}^d = (z_{i1}^d, z_{i2}^d, z_{i3}^d, z_{i4}^d)^T$ is the desired state of follower robots R_{i} in chained form, respectively.

Based on equations (13) and (14), the error differential equations are given as follows

$$\begin{cases} \dot{z}_{i1e} = u_{i1} - u_{i1}^d \\ \dot{z}_{i2e} = u_{i2} - u_{i2}^d \\ \dot{z}_{i3e} = z_{i2e}u_{i1}^d + z_{i2}(u_{i1} - u_{i1}^d) \\ \dot{z}_{i4e} = z_{i3e}u_{i1}^d + z_{i3}(u_{i1} - u_{i1}^d) \end{cases} \tag{15}$$

Then, we need to find a Lipschitz continuous time-varying state-feedback controller $\tilde{u}_i = \begin{bmatrix} u_{i1} \\ u_{i2} \end{bmatrix} = \tilde{u}(Z_{ie}, u_{i1}^d, u_{i2}^d)$ for follower robots R_{i} to make the tracking error Z_{ie} converge to zero, asymptotically, that is, $Z_{ie} = \lim_{t\to\infty} |Z_i^d - Z_i| = 0$ under appropriate conditions on the reference control functions u_{i1}^d and u_{i2}^d.

Next, we introduce a change of coordinates and rearrange the system (15) into a triangular-like form so that the integrator backstepping can be applied.

Denote $\tilde{x}_d := (x_{2d}, x_{3d})$ and let $\Phi_1(\cdot; x_d) : R^4 \to R^4$ be the mapping defined by

$$\begin{cases} \xi_{i1} = z_{i4e} - (z_{i3e} + z_{i3}^d) \cdot z_{i1e} \\ \xi_{i2} = z_{i3e} - (z_{i2e} + z_{i2}^d) \cdot z_{i1e} \\ \xi_{i3} = z_{i2e} \\ \xi_{i4} = z_{i1e} \end{cases} \tag{16}$$

In the new coordinates $\xi_i = (\xi_{i1}, \xi_{i2}, \xi_{i3}, \xi_{i4})$, equation (15) is transformed into

$$\begin{cases} \dot{\xi}_{i1} = u_{i1}^d \xi_{i2} - z_{i2}(u_{i1} - u_{i1}^d)\xi_{i4} \\ \dot{\xi}_{i2} = u_{i1}^d \xi_{i3} - u_{i1}^d \xi_{i4} \\ \dot{\xi}_{i3} = u_{i2} - u_{i2}^d \\ \dot{\xi}_{i4} = u_{i1} - u_{i1}^d \end{cases} \tag{17}$$

The transformation of tracking error model has been transformed into a triangular-like form, and then we formulate our backstepping design scheme for this new system (17).

Trajectory tracking controller design based on backstepping method

The basic idea for trajectory tracking controller design based on backstepping is a recursive design.[13] The complex system is divided into lower dimension subsystems, then the Lyapunov function and intermediate virtual control inputs are recursively designed for every subsystem. The recursive design proceeds until backstepping has been achieved by the whole system. Finally, the actual control input achieves the original design objective.

Step 1: Based on the study by Jiang and Nijmeijer, [13] start with the ξ_{i1}-subsystem of equation (17)

$$\dot{\xi}_{i1} = u_{i1}^d \xi_{i2} - z_{i2}(u_{i1} - u_{i1}^d)\xi_{i4} \tag{18}$$

We consider the variable ξ_{i2} as a virtual control input and the variables u_{i1}^d and ξ_{i4} are considered as the time-varying functions.

Set $\overline{\xi_{i1}} = \xi_{i1}$. Along the solutions of equation (17), the time derivative of the positive definite and proper function $V_{i1}(\overline{\xi_{i1}}) = \frac{1}{2}\overline{\xi_{i1}}^2$ satisfies $\dot{V}_{i1} = \bar{\xi}_{i1}\xi_{i2}u_{i1}^d - \bar{\xi}_{i1}z_{i2}(u_{i1} - u_{i1}^d)\xi_{i4}$

Observe that $g_{i1}(\bar{\xi}_{i1}) = 0$ is a stabilizing function for equation (18), whenever $\xi_{i4} = 0$. We introduce a new variable $\bar{\xi}_{i2}$ as $\bar{\xi}_{i2} = \xi_{i2} - g_{i1}(\xi_{i1})$.Then, equation (18) yields $\dot{V}_{i1} = \bar{\xi}_{i1}\bar{\xi}_{i2}u_{i1}^d - \bar{\xi}_{i1}z_{i2}(u_{i1} - u_{i1}^d)\xi_{i4}$.

Step 2: Consider the (ξ_{i1}, ξ_{i2})-subsystem of equation (17), and choose the positive definite and proper function $V_{i2}(\bar{\xi}_{i1}, \bar{\xi}_{i2}) = V_{i1} + \frac{1}{2}\bar{\xi}_{i2}^2$, which satisfies

$$\begin{aligned} \dot{V}_{i2} &= \dot{V}_{i1} + \bar{\xi}_{i2} \cdot \dot{\bar{\xi}}_{i2} = {u_{i1}}^d \bar{\xi}_{i2}(\bar{\xi}_{i1} + \xi_{i3}) \\ &\quad - \bar{\xi}_{i1}z_{i2}(u_{i1} - u_{i1}^d)\xi_{i4} - \bar{\xi}_{i2}u_{i2}\xi_{i4} \end{aligned}$$

where $\bar{\xi}_{i2} = \xi_{i2} - g_{i1}(\xi_{i1})$, view ξ_{i3} as the virtual control input, the expected value is g_{i2}, defining $\bar{\xi}_{i3} = \xi_{i3} - g_{i2}(\xi_{i1}, \xi_{i2})$ which satisfies

$$\begin{aligned}\dot{\bar{\xi}}_{i2} &= \dot{\xi}_{i2} - \frac{\partial g_{i1}}{\partial \xi_{i1}} \cdot \dot{\xi}_{i1} \\ &= \dot{\xi}_{i2} \\ &= u_{i1}^d \xi_{i3} - u_{i2}\xi_{i4} \\ &= u_{i1}^d(\xi_{i1} + \xi_{i3}) - u_{i2}\xi_{i4} - u_{i1}^d \xi_{i1} \\ &= u_{i1}^d\left(\xi_{i3} - g_{i2}(\xi_{i1}, \xi_{i2})\right) - u_{i2}\xi_{i4} - u_{i1}^d \xi_{i1}\end{aligned}$$

Thus, $g_{i2}(\xi_{i1}, \xi_{i2}) = -\xi_{i1}$ and the derivation of $\bar{\xi}_{i3}$ is

$$\begin{aligned}\dot{\bar{\xi}}_{i3} &= \dot{\xi}_{i3} - \left(\frac{\partial g_{i2}}{\partial \xi_{i1}} \cdot \dot{\xi}_{i1} + \frac{\partial g_{i2}}{\partial \xi_{i2}} \cdot \dot{\xi}_{i2}\right) \\ &= \dot{\xi}_{i3} - (-\dot{\xi}_{i1}) \\ &= u_{i2} - u_{i2}^d + u_{i1}^d \xi_{i2} - z_{i2}(u_{i1} - u_{i1}^d)\xi_{i4}\end{aligned}$$

Step 3: Consider $(\dot{\bar{\xi}}_{i1}, \dot{\bar{\xi}}_{i2}, \dot{\bar{\xi}}_{i3})$ subsystem of equation (17), and choose the positive definite and proper function $V_{i3}(\bar{\xi}_{i1}, \bar{\xi}_{i2}, \bar{\xi}_{i3}) = V_{i2} + \frac{1}{2}\bar{\xi}_{i3}{}^2$, which satisfies

$$\begin{aligned}\dot{V}_{i3} &= \dot{V}_{i2} + \bar{\xi}_{i3}\dot{\bar{\xi}}_{i3} \\ &= (u_{i1}^d \bar{\xi}_{i2} + \xi_{i2} - u_{i1}^d + u_{i1}^d z_{i2})\bar{\xi}_{i3} \\ &\quad - z_{i2}(\bar{\xi}_{i1} + \bar{\xi}_{i3})(u_{i1} - u_{i1}^d)\xi_{i4} - u_{i2}\bar{\xi}_{i2}\xi_{i4}\end{aligned}$$

In order to make $\dot{V}_{i3}$ negative definite, we choose

$$-k_1\bar{\xi}_{i3} = u_{i1}^d \bar{\xi}_{i2} + u_{i2} - u_{i2}^d + u_{i1}^d \xi_{i2} \tag{19}$$

where $k_1 > 0$, thus

$$u_{i2} = u_{i2}^d - 2u_{i1}^d \xi_{i2} - k_1(\xi_{i1} + \xi_{i3}) \tag{20}$$

Step 4: Consider $(\dot{\xi}_{i1}, \dot{\xi}_{i2}, \dot{\xi}_{i3}, \dot{\xi}_{i4})$-subsystem of equation (17), and choose the Lyapunov function $V_{i4}(\bar{\xi}_{i1}, \bar{\xi}_{i2}, \bar{\xi}_{i3}, \bar{\xi}_{i4}) = V_{i3} + \frac{1}{2}\bar{\xi}_{i4}^2$, which satisfies

$$\begin{aligned}\dot{V}_{i4} &= \dot{V}_{i3} + \bar{\xi}_{i4}\dot{\bar{\xi}}_{i4} \\ &= -k_1\bar{\xi}_{i3}{}^2 + [(1 - z_{i2}\bar{\xi}_{i1} - z_{i2}\bar{\xi}_{i3}) \cdot (u_{i1} - u_{i1}^d) \\ &\quad - u_{i2}\bar{\xi}_{i2}]\xi_{i4}\end{aligned}$$

To make $\dot{V}_{i4}$ negative definite, choose

$$-k_2\xi_{i4} = \left(1 - z_{i2}\bar{\xi}_{i1} - z_{i2}\bar{\xi}_{i3}\right)\left(u_{i1} - u_{i1}^d\right) - u_{i2}\bar{\xi}_{i2} \tag{21}$$

where $k_2 > 0$, thus

$$u_{i1} = u_{i1}^d + \frac{(u_{i2}\xi_{i2} - k_2\xi_{i4})}{(1 - 2\xi_{i1}z_{i2} - z_{i2}\xi_{i3})} \tag{22}$$

In conclusion, we get the Lipschitz continuous time-varying state-feedback controller, which is in chained form

$$\begin{cases} u_{i1} = u_{i1}^d + \dfrac{(u_{i2}\xi_{i2} - k_2\xi_{i4})}{(1 - 2\xi_{i1}z_{i2} - z_{i2}\xi_{i3})} \\ u_{i2} = u_{i2}{}^d - 2u_{i1}{}^d\xi_{i2} - k_1(\xi_{i1} + \xi_{i3}) \end{cases} \tag{23}$$

where $u_{i1}^d = \nu_i^d \cos(\theta_i^d + \phi_i^d)$

$$\begin{aligned}u_{i2}{}^d = &\frac{[3\sin\phi_i^d \sin(\theta_i^d + \phi_i^d)\sec^4(\theta_i^d + \phi_i^d) + \cos\phi_i^d \sec^3(\theta_i^d + \phi_i^d)] \cdot \omega_i^d}{d} \\ &+ \frac{3\sin(\theta_i^d + \phi_i^d)\sin^2\phi_i^d \sec^4(\theta_i^d + \phi_i^d) \cdot \nu_i^d}{d^2}\end{aligned}$$

$$\xi_{i1} = y_i - y_i^d - \tan(\theta_i + \phi)_i \cdot (x_i - x_i^d)$$

$$\xi_{i2} = \tan(\theta_i^d + \phi_i^d) - \tan(\theta_i + \phi_i) - \frac{1}{d}\sin\phi_i \sec^3(\theta_i + \phi_i) \cdot (x_i - x_i^d)$$

$$\xi_{i3} = \frac{1}{d}[\sin\phi_i{}^d \sec^3(\theta_i^d + \phi_i^d) - \sin\phi_i \sec^3(\theta_i + \phi_i)]$$

$$\xi_{i4} = x_i - x_i^d$$

$$z_{i2} = \frac{1}{d}\sin\phi_i \sec^3(\theta_i + \phi_i^d)$$

We should change it into the control inputs, based on equations (8) and (23), we get the control inputs $[\nu_i, \omega_i]^T$ of follower robot R_i

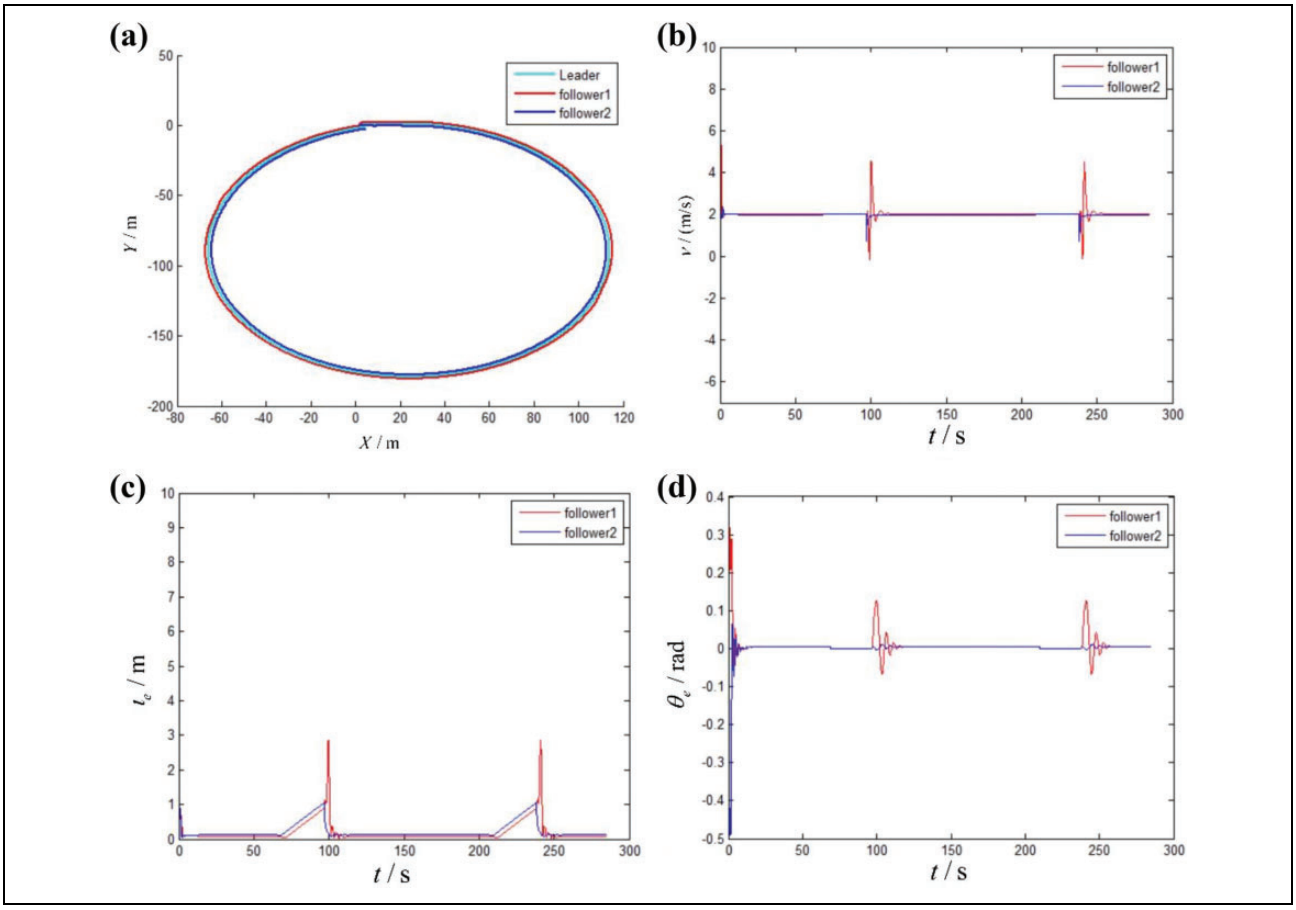

Figure 4. Circle trajectory of the leader robot with two follower robots to realize a triangular formation. (a) Circle trajectory of the formation; (b) linear velocity of follower robots; and (c) and (d) position error and the heading angle error of follower robots, respectively.

$$\begin{cases} \nu_i = \dfrac{u_{i1}}{\cos(\theta_i + \phi_i)} \\ \omega_i = \dfrac{u_{i2}d^2 - 3\sin(\theta_i + \phi_i)\sin^2\phi_i \sec^4(\theta_i + \phi_i) \cdot \nu_i}{d^2[3\sin\phi_i \sin(\theta_i + \phi_i)\sec^4(\theta_i + \phi_i) + \cos\phi_i \sec^3(\theta_i + \phi_i)]} \end{cases} \tag{24}$$

$[\nu_i, \omega_i]^T$ is the tracking controller, which is the linear velocity and steering velocity inputs of the nonholonomic car-like robot, respectively, designed by chained form system and backstepping methods to make the follower robots achieve the formation precisely without front-wheel being jammed.

Results and discussions of the simulations and experiments

Simulations of circle trajectory tracking of leader–follower formation

To validate the effectiveness of the proposed tracking controller, we consider three robots forming a typical triangle formation, composed of a leader robot R_L and two follower robots R_1 and R_2 with the desired distances $l_{1L}^d = 1.9$ m and $l_{2L}^d = 1.9$ m, and the desired bearing angles $\varphi_{1L}^d = 45^\circ$ and $\varphi_{2L}^d = 45^\circ$. The position error of the follower robot is $\iota_e = \sqrt{x_e{}^2 + y_e{}^2}$, and the heading angle error is θ_e. The distance from the rear axle to the front of each robot is $d = 0.5$ m.

Figure 4 shows the leader robot performing a circle path which starts from the initial posture at $(2,\ 1,\ 30^\circ,\ -0.01)^T$, where the desired linear velocity is $v_L = 5$ m/s and the angular velocity is $\omega_L = 0.01$ rad/s. The follower 1 starts from the initial posture $(1.5,\ 1.5,\ -15^\circ,\ 45^\circ)^T$ and follower 2 starts from the initial posture $(1.5,\ 0.5,\ -15^\circ,\ -45^\circ)^T$, respectively.

The controller's parameters in equation (24) are chosen as $k_1 = 2.3$ and $k_2 = 1.3$.

The proposed control algorithms make the three robots move to form the formation. When $t = 100$ s and $t = 200$ s (in Figure 4(b)), we can see the velocity of follower 1 changes fast, which is caused by the denominator being nearly zero in equation (24). The phenomenon of front-wheel being jammed does not occur during the forming, and follower robots, finally, achieve the triangle-like formation. The trajectory tracking errors of follower robots are shown in Figure 4(c) and (d). We can observe when $t = 100$ s and $t = 200$ s, that is, at the quarter of a circle, the front wheels turn 90°, oscillations occur, which is caused by the denominator being nearly zero in equation (24), and the phenomenon of front-wheel being jammed does not occur. After this, the trajectory tracking errors can quickly converge to zero.

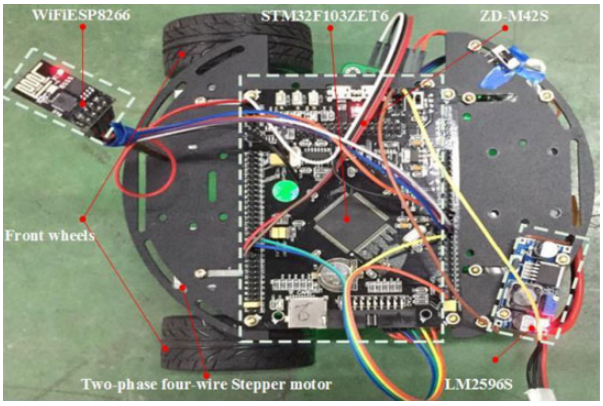

Figure 5. The prototype of the car-like robot with front-wheel driving and steering.

Prototype experiments

We made an experiment of circle trajectory tracking of the leader robot with two follower robots to realize a triangular formation. The prototype of the novel car-like robot with front-wheel driving and steering is shown in Figure 5. We show the effectiveness of three front wheel-driving and steering mobile robots with the newly designed controller

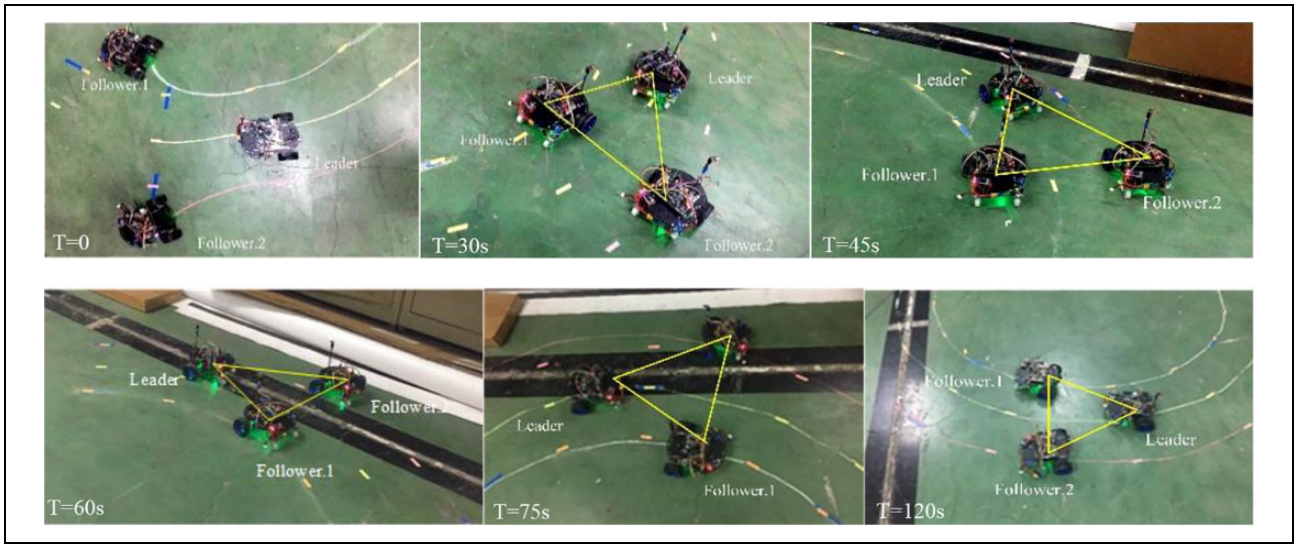

Figure 6. Snapshots of the video about circle trajectory of the leader robot with two follower robots to realize a triangular formation (supplementary video associated with this article can be found in the Online Supplementary Material.)

Table 1. Experiment data of circle trajectory of the leader robot with two follower robots.

Time (s)	Leader.x (m)	Leader.y (m)	Follower1.x (m)	Follower1.y (m)	Follower2.x (m)	Follower2.y (m)
$T = 0$	1.10	1.05	0.84	0.63	1.49	0.73
$T = 15$	1.39	1.78	0.92	1.33	1.38	1.39
$T = 30$	2.03	2.07	1.54	2.17	1.71	1.81
$T = 45$	2.81	1.81	2.53	2.21	2.37	1.12
$T = 60$	2.98	1.12	3.31	1.55	2.83	1.46
$T = 75$	2.82	0.38	3.12	0.61	2.70	0.78
$T = 90$	2.11	0.08	2.49	-0.12	2.45	0.38
$T = 105$	1.45	0.32	1.55	-0.07	1.82	0.32
$T = 120$	1.12	0.95	0.92	0.61	1.29	0.68

to demonstrate the formation control performance. The three robots communicate and share data via wireless communication and the robot localizes itself by odometry.

We made an experiment of circle trajectory tracking of leader–follower formation in Figure 6. The leader robot performing a circle path which starts from the initial position at $(1.10,\ 1.05,\ 30^\circ,\ -0.01)^T$, with the desired linear velocity is $v_L = 0.8$ m/s and the angular velocity is $\omega_L = 0.4$ rad/s. The follower 1 starts from the initial posture at $(0.84,\ 0.63,\ -15^\circ,\ 45^\circ)^T$, and follower 2 starts from the initial posture at $(1.49,\ 0.73,\ -15^\circ,\ -45^\circ)^T$. The controller's parameters in equation (24) are chosen as $k_1 = 2.3$ and $k_2 = 1.3$. We choose some point on the floor to establish an inertial Cartesian frame and we get the data of the formation in Table 1.

The proposed controller makes the robots move to form and maintain the triangle formation, and when $t = 30$ s, they nearly form the predefined triangular formation from the initial states. During the forming and maintaining, the phenomenon of jamming does not occur. However, during the moving process, communication appears delays, and sometimes the follower robots receive the wrong data, even receives nothing.

Conclusions

This work aims to solve the problem of the conventional car-like robots, with front wheels steering and rear wheels driving, may be jammed at the front wheels angle nearly 90° during the formation forming. We propose a novel car-like robot with the integration of front-wheel driving and steering and employed it in the leader–follower formation control.

Considering the characteristics of the robot, the new car-like robot has a different kinematic model from the conventional one, we establish its kinematic model and analyze its controllability via the method of chained form system. Based on this, we design the trajectory-tracking controller for the novel robots to form the formation via the backstepping method. Finally, we do the simulations and experiments to validate our algorithm and the phenomenon of jamming does not occur during the formation forming.

This is a complete and constructive work, which contains robot's driving mode redesign, kinematic model establishment, controllability analysis, and formation controller design. In addition, this novel car-like robot with the integration of front-wheel driving and steering system not only avoids the jamming in the formation motion, but also owes the advantages of compacter structure, lighter body, and lower energy consumption. This work can provide guidelines and references for the design of unmanned ground vehicles and multi-robot formation.

When the new robot performs tasks with requirements of high speed and/or transport of heavy loads, such tasks exert external forces on the robot and will inevitably influence its trajectory tracking. Thus, our kinematic model in this article is not sufficient. Dynamic characteristics of the mobile robot, such as mass and inertia center, need to be considered in our future work. In addition, the communication delay may occur during the multi-robot formation motion, which results in formation distortion or costs more time reforming the formation. To make the formation more effective, the problem of communication delay needs to be solved in the future.

Declaration of conflicting interests

The author(s) declared no potential conflicts of interest with respect to the research, authorship, and/or publication of this article.

Funding

The author(s) disclosed receipt of the following financial support for the research, authorship, and/or publication of this article: This research has been supported by the National Natural Science Foundation, China (no. 51775435), and the Programme of Introducing Talents of Discipline to Universities (B13044).

Supplemental material

Supplementary material for this article is available online.

References

1. Oh H, Shirazi AR, Sun CL, et al. Bio-inspired self-organising multi-robot pattern formation: a review. *Robot Auto Syst* 2017; 91: 83–100.
2. Arrichiello F, Chiaverini S, Indiveri G, et al. The null-space-based behavioral control for mobile robots with velocity actuator saturations. *Int J Robot Res* 2010; 29(10): 1317–1337.
3. Sadowska A, van den Broek T, Huijberts H, et al. A virtual structure approach to formation control of unicycle mobile robots using mutual coupling. *Int J Control* 2011; 84: 1886–1902.
4. Cruz-Morales RD, Velasco-Villa M, Castro-Linares R, et al. Leader-follower formation for nonholonomic mobile robots: discrete-time approach. *Int J Adv Robot Syst* 2016; 13(2): 12.
5. Chen XH and Jia YM. Input-constrained formation control of differential-drive mobile robots: geometric analysis and optimisation. *IET Contr Theory Appl* 2014; 8: 522–533.
6. Vidal R, Shakernia O and Sastry S. Formation control of nonholonomic mobile robots with omnidirectional visual servoing and motion segmentation. In: *20th IEEE international conference on robotics and automation (ICRA), Vols 1–3, Proceedings*, Taipei, Taiwan, 14–19 September 2003, pp. 584–589. IEEE.
7. Max G and Lantos B. Adaptive formation control of autonomous ground vehicles in leader-follower structure. In: *Proceedings paper 17th IEEE international symposium on computational intelligence and informatics (CINTI)*, Budapest, Hungary, 17–19 November 2016, pp. 13–18. IEEE.

8. Hwang CL. Comparison of path tracking control of a car-like mobile robot with and without motor dynamics. *IEEE-ASME Trans Mechatron* 2016; 21(4): 1801–1811.
9. Sadowska A and Huijberts H. Formation control design for car-like nonholonomic robots using the backstepping approach. *In: Proceedings paper European control conference (ECC)*, Zurich, 17–19 July 2013, pp. 1274–1279. IEEE.
10. Kumar U and Sukavanam N. Backstepping based trajectory tracking control of a four wheeled mobile robot. *Int J Adv Robot Syst* 2008; 5(4): 403–410.
11. Meng Q, Zhang T, He JF, et al. Adaptive vector sliding mode fault-tolerant control of the uncertain Stewart platform based on position measurements only. *Robotica* 2016; 34(6): 1297–1321.
12. Du HB, Wen GH, Yu XH, et al. Finite-time consensus of multiple nonholonomic chained-form systems based on recursive distributed observer. *Automatica* 2015; 62: 236–242.
13. Jiang ZP and Nijmeijer H. A recursive technique for tracking control of nonholonomic systems in chained form. *IEEE Trans Autom Control* 1999; 44(2): 265–279.
14. Nakamura Y, Ezaki H, Tan Y, et al. Design of steering mechanism and control of nonholonomic trailer systems. *IEEE Trans Robot Autom* 2001; 17(1): 367–374.
15. He G, Zhang C, Sun W, et al. Stabilizing the second-order nonholonomic systems with chained form by finite-time stabilizing controllers. *Robotica* 2016; 34(10): 2344–2367.